Available online at www.sciencedirect.com

SciVerse ScienceDirect

Ceramics International 39 (2013) 6441–6447

CERAMICS INTERNATIONAL

www.elsevier.com/locate/ceramint

High-current measurement of the grain resistivity in zinc oxide varistor ceramics

A.I. Ivon[a,*], R.I. Lavrov[a], A.B. Glot[b]

[a]Department of Physics, Electronics and Computer Systems, Dnepropetrovsk National University, 49010 Dnepropetrovsk, Ukraine
[b]Universidad Tecnològica de la Mixteca, Huajuapan de León, 69000 Oaxaca, Mexico

Received 15 December 2012; received in revised form 22 January 2013; accepted 23 January 2013
Available online 31 January 2013

Abstract

A new pulse technique for grain resistivity measurement in varistor ceramics is suggested. Such technique allows obtaining more precise value of the grain resistivity due to the use of the concept of differential electrical resistance. This technique can be used in the current density range where the overheating of varistor sample is insignificant. The technique was verified using commercial ZnO varistors. Grain resistivities of $0.60 \pm 0.02\ \Omega$ cm at 293 K and of $3.40 \pm 0.13\ \Omega$ cm at 77 K were obtained. This result indicates the negative temperature coefficient of grain resistance in ZnO varistor in the range (77–293) K. The contribution of the grain boundaries to the current–voltage characteristic of ZnO varistor is estimated on the basis of the measured grain resistivity and the current–voltage data. It is shown that the electrical conduction in ZnO varistor is controlled by grains if the current density exceeds approximately 1000 A cm^{-2}.

Keywords: A. Grain boundaries; C. Electrical properties; D. ZnO; E. Varistors

1. Introduction

ZnO-based ceramic materials with small additives of some oxides are widely used as varistors [1–4]. Such varistor ceramics contain highly conductive grains of doped ZnO with highly resistive grain boundaries due to the formation of the grain-boundary potential barriers during sintering in the oxidizing atmosphere [1–5].

The current–voltage ($I(U)$) characteristic of a varistor in the range of approximately (10^{-7}–10) A cm^{-2} can be described by the following empirical expression:

$$I = BU^{\beta} \tag{1}$$

where I is the current, U is the voltage, B is a constant and β is the nonlinearity coefficient. A high β value (~ 50) in varistors became the reason of their wide application for protection of different electrical equipment against overvoltage [1–4]. At low currents (below approximately 10^{-9} A cm^{-2}) β is decreased up to $\beta = 1$ because the Ohmic conduction dominates. In the high-current region ($J > 10$ A cm^{-2}) β is decreased too because the nonlinear electrical resistance of the grain boundaries becomes comparable with the linear electrical resistance of grains. As a result, a part of the applied voltage drops at the grain resistance, β value is decreased and the upturn region of $I(U)$ characteristic appears. Electrical properties of ZnO varistors at low currents strongly depend on their microstructure [6–8]. For example, the control of the grain size is important for improving the electrical homogeneity of varistor ceramics [6,7]. However, for applications of ZnO varistors as protecting devices, the high-current performance is important and the grain resistivity control is necessary.

The grain resistivity in commercial ZnO varistors is below 1 Ω cm [3,9–11]. If the grain resistivity is decreased, the upturn region of $J(E)$ characteristic appears at higher current densities. Therefore, the decrease of the grain resistivity ρ_g in ZnO varistors is an important practical problem [2–4,9–11]. Additionally, to interpret some phenomena observed at high currents in ZnO varistors it would be useful to know a precise value of the grain resistivity [12,13]. The information about

*Corresponding author. Tel.: +380 056 760 94 57; fax: +380 056 374 98 41.
E-mail addresses: a_ivon@mail.ru, iai49@i.ua (A.I. Ivon).

0272-8842/$ - see front matter © 2013 Elsevier Ltd and Techna Group S.r.l. All rights reserved.
http://dx.doi.org/10.1016/j.ceramint.2013.01.072

the grain resistivity is useful also for the optimization of high-current properties of new varistors [14-16].

It should be mentioned that the measurement of the grain resistivity is very important for development of the high-quality SnO_2 varistors [16,17]. While earlier known SnO_2 varistors exhibited the grain resistivity (at 300 K) of the order of several $\Omega \cdot$ cm or higher [18–21], recently it was reported about SnO_2 varistors with ρ_g values comparable with the grain resistivity in ZnO varistors [17]. Recently reported SnO_2 varistors with a high energy absorption capability [22,23] exhibit relatively low grain resistivity: it is estimated as 0.5 Ω cm in Ref. [23] and it can be assumed that the grain resistivity in other case [22] is the same order of magnitude.

Therefore, the measurement of the grain resistivity is a necessary task at the manufacture and research of ZnO and SnO_2 varistors. The estimation of the grain resistivity can be performed using the dielectric spectroscopy [9,24,25], the infrared reflectance [10] and the high-current pulses [9,11,26]. However, the accuracy of all these measurements is rather not very high. The approximate estimation of the grain resistivity in ZnO ceramics after the electrical breakdown was performed in Ref. [27]. However, in this case the error can be significant because the breakdown occurs in the narrow channel (much less than the sample cross-section) and, of course, this technique is not non-destructive.

The high-frequency [9,25] and optical [10] methods give rather a rough estimation of ρ_g. In Ref. [25] the grain resistivity and its temperature dependence were estimated using the high-frequency parameters of ZnO varistors. However, the absence of the experimental spectra at different temperatures makes results and conclusions in Ref. [25] not sufficiently convincing. The pulse method is more reliable because it is directly related to the conduction process at high currents. According to the pulse technique [26], it is necessary to obtain nearly linear $E(J)$ relation in the range of $J > 1000$ A cm^{-2} by using several high-current single pulses with different amplitudes. The grain resistivity can be estimated from this relation as $\rho_g = \Delta E/\Delta J$, where ΔE is the increment of the electric field and ΔJ is the respective increment of the current density.

However, even at current densities higher than 1000 A cm^{-2} the $E(J)$ characteristic is not exactly linear due to some contribution of the voltage drop at the grain-boundary regions and the influence of a sample heating. This gives some error in the estimated value of the grain resistivity. Additionally, it should be mentioned that for some compositions of varistor ceramics it is difficult to reach a high-current linear region of the $E(J)$ dependence because of the irreversible electrical breakdown of a sample. It complicates the correct estimation of the grain resistivity. Thus, it can be concluded that known methods give only an estimation of the grain resistivity. Therefore, it would be desirable to develop a technique for the measurement of the grain resistivity in varistor ceramics which allows decreasing an overheating of a sample and finding the contribution of the grain boundaries to the $J(E)$ characteristic of varistor ceramics at high currents.

The purpose of this paper is the development of a pulse technique of the grain resistivity measurement in varistor ceramics avoiding the use of extremely high-current pulses. Such technique should give a relatively precise value of the grain resistivity. Using a measured value of the grain resistivity and the $I(U)$ data for a given varistor, it will be possible to obtain a contribution of the grain-boundary regions to the current–voltage characteristic of the varistor at high electric currents.

2. Material and methods

Commercial zinc oxide varistors (CH2-1, Russia) were used for the measurements. This material contains approximately 97 mol% ZnO and Bi_2O_3, Sb_2O_3, Co_3O_4, Cr_2O_3, MnO_2, as additives.

The current–voltage characteristics in the range of dc current (10^{-13}–10^{-2}) A were obtained using the whole varistor disc 16.5 mm in diameter and 1 mm in thickness (the diameter of Ag electrodes was 14 mm).

In this paper the current density in the range (30–500) A cm^{-2} was used for the measurement of the grain resistivity. The samples with a small electrode area were utilized for reaching a high current density in the range (10^{-2}–10^{4}) A cm^{-2}. The use of such samples is not compulsory for the suggested technique because these experiments can also be performed using standard samples 16.5 mm in diameter and respective pulse generator. However, the measurements can be conducted in different parts of a ceramic sample if a small electrode area is used. This way an additional information about the electrical homogeneity of a ceramic sample at high currents can be obtained.

The samples with a small electrode area were prepared the next way. Small dots of lacquer were applied at carefully selected points in the hexagonal configuration on both original Ag surfaces. Due to a wetting the shape of lacquer dots was nearly circle with diameter in the range of (1.7–2.0) mm. After drying of lacquer, the uncoated parts of electrode were etched in 30 wt% HNO_3 to remove the unprotected silver. Then lacquer was eliminated by an appropriate solvent. The diameter of each Ag spot was measured using an optical microscope. The square of electrodes was in the range of (0.023–0.030) cm^2. Thus, from one varistor disk with electrodes we have obtained many samples with a small electrode area. Fig. 1a illustrates the obtained electrode configuration at the surfaces of a varistor disc. The displacement between the centers of electrode areas at both sides of the same small sample was less than 0.3 mm. The distance between the edges of the neighbor electrodes was not less than 3 mm. It excepted the influence of neighbor electrodes during the pulse measurements. The varistor disk was put into the transformer oil to avoid discharges in air during the pulse measurements.

The current–voltage characteristics of the whole varistor disc and different small samples in the scale $J(E)$ were practically the same. Therefore, the studied ceramic material is quite electrically homogeneous at low and high currents.

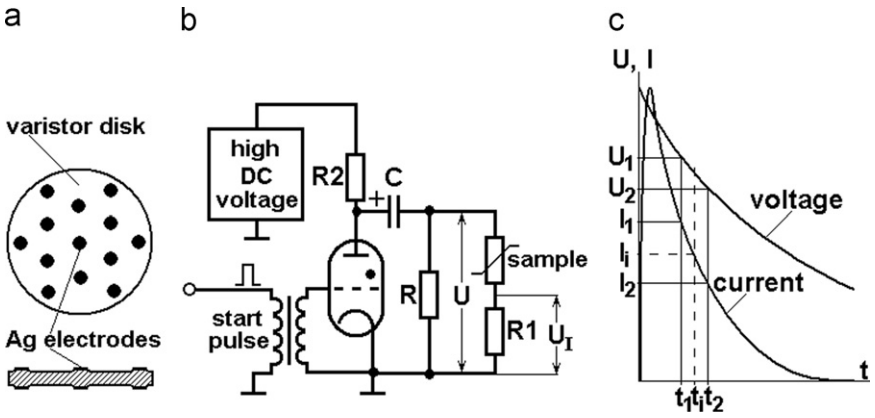

Fig. 1. The electrode configuration used for the high-current pulse study (a), the circuit for the formation of a single exponential voltage pulse (b) and the explanation how the voltage, the current and the differential resistance are calculated from the oscillograms (c).

The current–voltage characteristic at high currents was obtained using a single exponential voltage pulse:

$$U(t) = U_0 \exp(-t/\tau) \quad (2)$$

where U_0 is the voltage amplitude, t is the time, τ is the time constant. Such a pulse is formed using the circuit shown in Fig. 1b. The short low-voltage start pulse causes a discharge of a capacitor with the capacitance C through a non-inductive resistor with resistance $R = 3\ \Omega$. The tested varistor sample was connected in series to the precision resistor R1 = 1 Ω and they were connected in parallel to the resistor R. The waveforms of $U(t)$ (“voltage”) and $U_I(t)$ (“current”) were recorded (see Fig. 1b) using the dual-channel storage oscilloscope C8-11. The value of current I through the varistor sample was determined as the voltage drop U_I at the precision resistor R1—$I = U_I/R1$. The voltage drop at the varistor sample was determined as the difference between the voltages at R and R1—U–U_I.

The circuit in Fig. 1b can form a single exponential voltage pulse with the time constant in the range 70–4000 μs at the change in a value of capacitor C. It is necessary to mention that for correct measurement of the grain resistivity, the shape of the voltage pulse must not be influenced by the tested sample. It occurs if the electrical resistance of the sample is much higher than R. The resistance of sample with small electrodes at high currents in the investigated range was at least 10 times higher than R.

The oscillograms of voltage and current ($U(t)$ and $U_I(t)$, see Fig. 1c) were used for plotting the current–voltage characteristics and the dependence of the differential resistance on current. Fig. 1c schematically shows the oscillograms of current and voltage and illustrates the calculation of the differential resistance $\Delta U/\Delta I$ on the basis of these oscillograms. Such oscillograms are actually the current–voltage characteristics in the parametric form with time t as a parameter. Each oscillogram of current and voltage allows obtaining several points at the current–voltage characteristic.

The increments of voltage and current ($\Delta U = U_1$–U_2 and $\Delta I = I_1$–I_2, respectively) can be found at a given moment of time t_i related to the current I_i. Then the differential resistance at current $I_i = (I_1 + I_2)/2$ is $\Delta U/\Delta I = (U_1$–$U_2)/(I_1$–$I_2)$. The expression for the differential resistance of a sample R_{dif} at current I can be obtained in such a form:

$$R_{dif} \cong R1((U_1 - U_2)/(U_{I1} - U_{I2}) - 1) \quad (3)$$

$$I = (U_{I1} + U_{I2})/(2R1) \quad (4)$$

The expressions for R_{dif} and I can be represented as specific parameters ρ_{dif} and J using the electrode area S and the thickness L.

For improvement of the measurement accuracy, the oscillograms of current and voltage were converted to a digital image. These images were processed with Adobe Photoshop CS and Microsoft Excel. As a result, the relative error was decreased to ±2%. For recording of the current–voltage characteristics, the voltage pulses with the time constant $\tau = 100$ μs were used. It allowed avoiding the irreversible electrical breakdown and minimizing a sample heating.

3. Results

The central idea of the suggested method is the determination of the grain resistance without reaching very high currents. For the explanation of the suggested method we use the equivalent circuit shown in Fig. 2a. The resistor R_g represents the bulk resistance of ZnO grains in varistor ceramics. The nonlinear resistance R_b is related to the grain boundaries where the double Schottky barriers are situated. The contribution of the barrier and grain capacitances is not taken into account in Fig. 2a due to the fact that the active current dominates over the reactive current in the high-current region ($J > 10\ A\ cm^{-2}$). Additionally, the time constant $\tau \sim 100$ μs of used exponential voltage pulse (see Eq. (2)) is significantly higher than the time constant of transient process related to mentioned capacitances.

Using Eq. (1), the voltage at a varistor $U = U_g + U_b$ can be written in the specific parameters:

$$E = J\rho_g + AJ^{1/\beta} \quad (5)$$

where $E = U/L$ is the average electric field strength in varistor; A is a constant depending on the constant B from Eq. (1), the electrode area S and the thickness of a sample

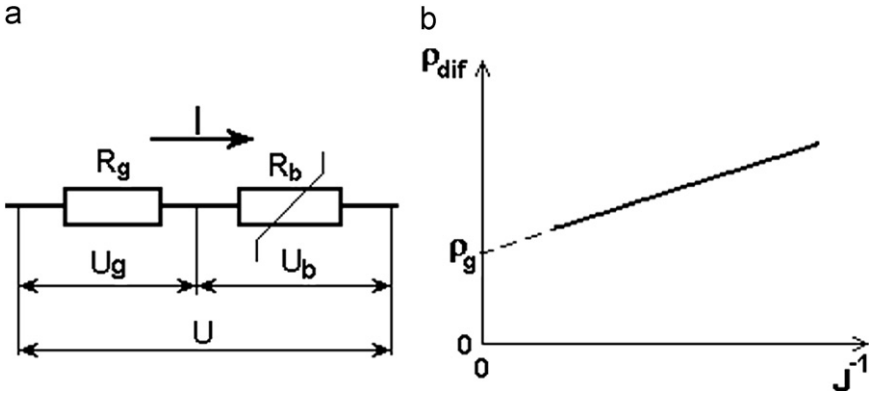

Fig. 2. The equivalent circuit for ZnO varistor (a) and the expected dependence of the differential resistivity of varistor ceramics as a function of the inverse current density (b).

L. Therefore, the differential resistivity $\rho_{dif}=dE/dJ$ can be obtained in the next form:

$$\rho_{dif}=\rho_g+AJ^{(1/\beta)-1}/\beta \quad (6)$$

Due to $\beta\gg1$ and, therefore, $1/\beta\ll1$, Eq. (6) can be written as:

$$\rho_{dif}=\rho_g+AJ^{-1}/\beta \quad (7)$$

It is seen from Eq. (7) that the differential resistivity depends linearly on the inverse electric current density J^{-1}. If we extrapolate the linear dependence ρ_{dif} (J^{-1}) to $J^{-1}=0$, then the grain resistivity ρ_g will be determined (Fig. 2b).

The oscillograms of current and voltage obtained at two temperatures are shown in Fig. 3. The oscillograms were recorded at the same charging voltage of the capacitor C (Fig. 1b). The horizontal line gives the zero signal level.

The current–voltage characteristics plotted from the oscillograms (Fig. 3) are shown in Fig. 4 (curves 1 and 3). The time step for plotting the current–voltage characteristics was 2 μs. The dependences of the differential resistivity on the inverse current density are presented in Fig. 5. The time step for calculation of the differential resistance was 6 μs. The experimental current–voltage characteristics of the investigated ZnO varistor ceramics in a wide current range are represented in the double logarithmic scale in Fig. 6.

4. Discussion

Three regions with different slopes (with different nonlinearity coefficients β) can be distinguished at the current–voltage characteristic in the double logarithmic scale (Fig. 6). Below approximately 10^{-9} A cm^{-2} the nonlinearity coefficient $\beta\cong1$ (Ohm's law takes place). The thermionic emission over the double Schottky barriers at the grain boundaries is responsible for the electrical conduction in this range. The highly nonlinear ($\beta\cong50$) part of the current–voltage characteristic in the range of approximately (10^{-8}–10) A cm^{-2} is caused by the band-to-band tunneling (Zener effect) [28–30] or impact ionization in the reverse-biased depletion layer [31,32]. Above approximately 10 A cm^{-2} a decrease in the slope of the current–voltage characteristic (in the nonlinearity coefficient) takes place (Fig. 6). It is due to the non-zero electrical resistance of grains connected in series to the grain-boundary regions where Schottky barriers are localized. The current–voltage characteristic obtained above approximately 10 A cm^{-2} (30–500 A cm^{-2}, see Section 2.) was used in present work for the measurement of the grain resistivity.

As it is seen from Fig. 5, the differential resistivity ρ_{dif} is decreased if the current is increased and the dependence of ρ_{dif} on J^{-1} is linear. This fact confirms Eq. (7). Then, extrapolation of the dependences ρ_{dif} (J^{-1}) (see Fig. 5) to a zero value of the inverse current density $(J^{-1}=0)$ gives the grain resistivity of $0.60\pm0.02\,\Omega$ cm at 293 K and of $3.40\pm0.13\,\Omega$ cm at 77 K. The method of least squares was used for the linear approximation in Fig. 5.

Consequently, the temperature coefficient of the grain resistivity $(1/\rho_g)(d\rho_g/dT)$ in ZnO varistor ceramics in the range of (77–300) K is negative. It corresponds to the published data [24,33]. Using the linear region of the $E(J)$ dependence, the values of the grain resistivity of 0.5–1.1 Ω cm in ZnO varistor ceramics with different additives were obtained [26]. Therefore, the data at 293 K obtained in this paper using suggested technique are in agreement with earlier published results [9–11,26].

As it is clear from Fig. 5, the variation in the differential resistivity in the range of the current density $(1000\le J<\infty)$ A cm^{-2} is less than 30% of its value $\rho_{dif}=\rho_g$ at $J\to\infty$. Therefore, in this current density region the relation $dE/dJ\cong\rho_g$ approximately takes place. From the last equation the linear dependence between J and E can be obtained:

$$E=E_0+\rho_gJ \quad (8)$$

where E_0 is related to the voltage drop at the grain boundary regions. Therefore, if $J>1000$ A cm^{-2}, then the $E(J)$ dependence in ZnO varistor ceramics is close to the linear one as it was assumed earlier in Ref. [26]. Such dependence for varistor ceramics is supported by the data presented in Fig. 7 (curve 1). If the linear $E(J)$ dependence is extrapolated to $J=0$, then $E_0=3030$ V cm^{-1} is obtained for the studied ceramic material.

The almost linear behavior of the $E(J)$ dependence of a varistor at $J>1000$ A cm^{-2} is a consequence of a high

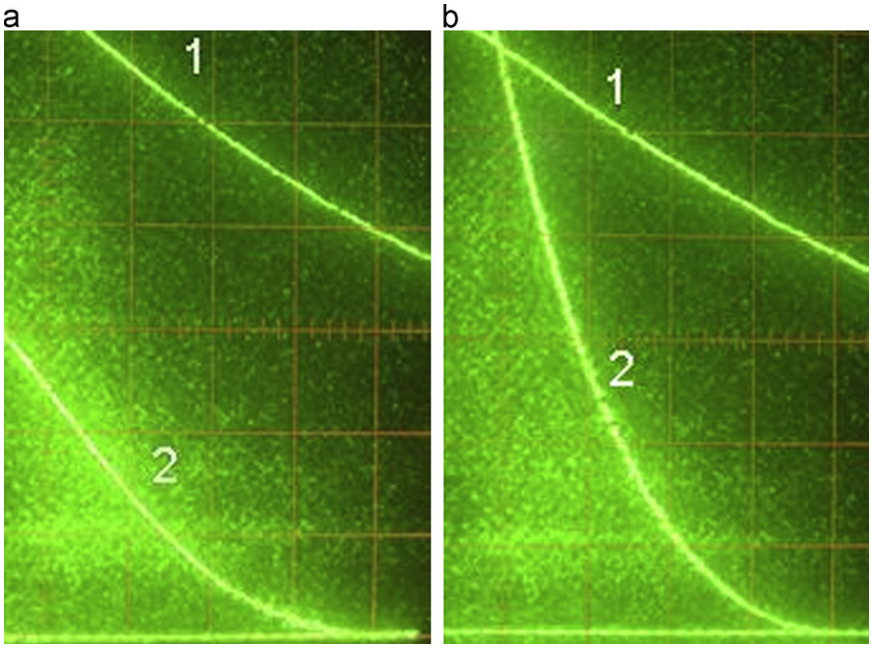

Fig. 3. The oscillograms of voltage (1) and current (2) at 77 K (a) and 293 K (b). The electrode area is 0.030 cm^2. Vertical: 82 V/div; 4.9 A/div. Horizontal: 10 μs/div.

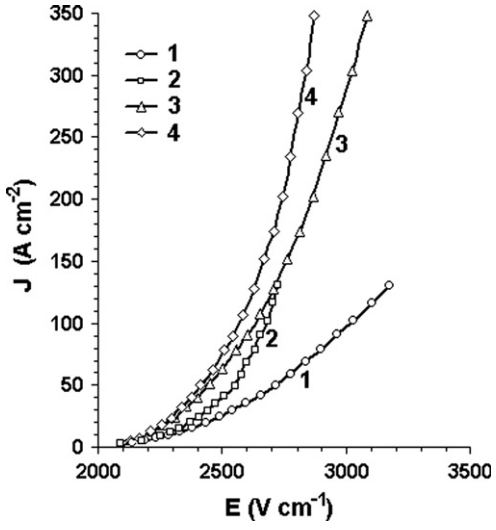

Fig. 4. The current–voltage characteristics of ZnO varistor ceramics (1,3) and the contributions of the grain boundaries to these characteristics (2,4) at 77 K (1,2) and 293 K (3,4).

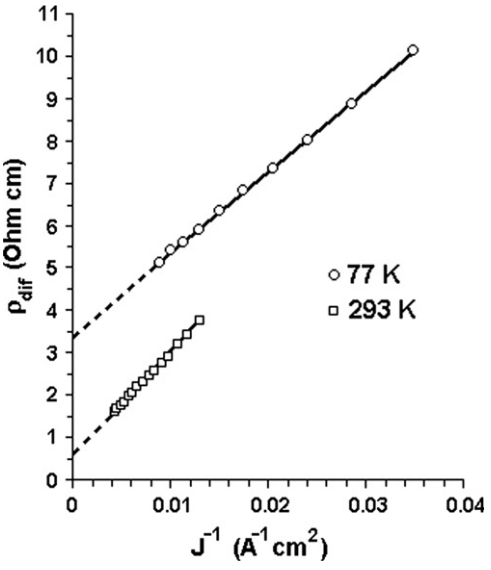

Fig. 5. The dependence of the differential resistivity on the inverse current density at 77 K and 293 K.

nonlinearity of the $J(E)$ characteristic of the grain boundaries with double Schottky barriers at high currents. In this case a considerable change in the current density leads to a weak change in the voltage drop at the grain boundaries. Therefore, the variation in the voltage drop at a sample is completely controlled by the linear resistance of the grains connected in series to the grain boundaries.

The value of the voltage drop at the individual barrier (3.3–3.6) V [34] satisfactorily correlates with the band gap of zinc oxide $E_{gap}=3.37$ eV [35]. Such a correlation is in accordance with the Zener effect [28–30] and impact ionization [31,32]. The high nonlinearity of the $I(U)$ characteristic in varistor ceramics for these mechanisms takes place if the voltage at the individual barrier is higher than $U_{b0} \cong E_{gap}/q$ (where q is the electron charge). In this connection, the constant E_0 in Eq. (8) can be considered as the average electric field in the ceramic sample for the initiation of the afore-mentioned nonlinearity mechanisms. If we assume that the same barriers are formed at all grain boundaries and the average grain size is l_g, then $U_{b0}=E_0 l_g$. Therefore, the average grain size l_g can be estimated from the experimental value of E_0 as $l_g \cong E_{gap}/(qE_0)$. The average size of ZnO grain estimated from the value $E_0=3030$ V cm^{-1} is 11 μm for the

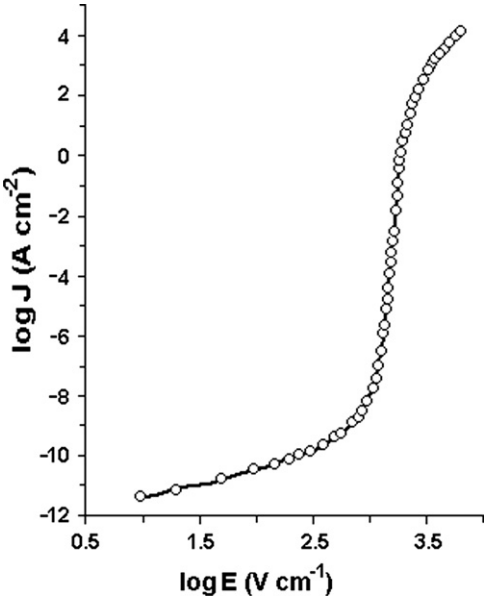

Fig. 6. The current–voltage characteristic of ZnO varistor ceramics in a wide current range at 295 K.

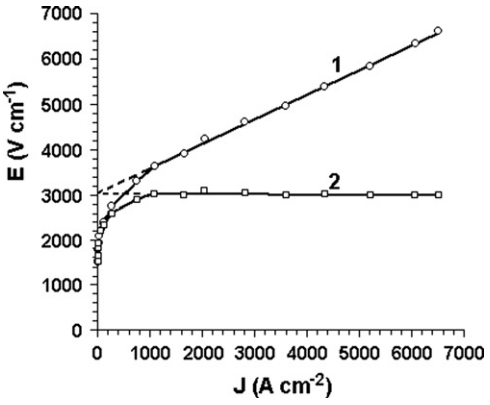

Fig. 7. The $E(J)$ relation for ZnO varistor ceramics (1) and the contribution of the grain boundaries (without grains) to this relation (2) at 295 K.

studied ceramic material. This value is in accordance with the optical microscopy data.

It would be interesting to separate the contributions of the grain boundaries and grains to the current–voltage characteristic of a ceramic sample at a high-current region. For this purpose, it is necessary to take into account that at any current the voltage drop at the sample is the sum of the barrier and the grain voltages $U=U_g+U_b$. Then, from the experimental relation $J(E)$ for the ceramic sample and the measured value of the grain resistivity ρ_g, the contribution of the grain boundaries $J=J(E_b)$ to the $J(E)$ dependence can be obtained. The value of E_b is calculated as $E_b=E-J\rho_g$, where $E_b=U_b/L$ is the contribution of the voltage drop at the grain boundaries (without grains) to the average electric field strength $E=U/L$. It should be mentioned that the actual electric field strength in the grain-boundary regions is much higher because the thickness of the grain-boundary barrier region is much lower than the grain size.

The contributions of the grain boundaries $J(E_b)$ to the current–voltage characteristics of ZnO varistor material $J(E)$ are represented in Fig. 4 (curves 2 and 4). They are displaced to the low-field region in comparison to the $J(E)$ relations for the varistor sample (curves 1 and 3 in Fig. 4). The increase in temperature from 77 K to 293 K causes a relatively weak (not more than 5%) shift of the $J(E_b)$ relation (in the range of 10 –350 A cm^{-2}) to the lower electric field.

In Fig. 7 the relations $E(J)$ in a wide current range are shown for ZnO varistor material (curve 1) and for the contribution of the grain boundaries (curve 2). It is seen that the voltage applied to the grain boundaries practically is not changed with current if the current density is higher than approximately 1000 A cm^{-2}. This voltage is related to the average electric field strength in ceramic sample $E_0=3030$ V cm^{-1}. Therefore, the electrical conduction in ZnO varistor is controlled by the grains if the current density is higher than approximately 1000 A cm^{-2}. The contribution of the grain-boundary regions to the $J(E)$ characteristic is observed as a parallel shift of this characteristic along the electric field axis by the value of $E_0=3030$ V cm^{-1}.

Therefore, the presented technique of the grain resistivity measurement in varistor ceramics additionally allows estimating the contribution of the grain boundaries (without grains) to the current–voltage characteristics what can be useful for the understanding of the non-Ohmic conduction nature in oxide varistor materials.

5. Conclusion

The modified pulse technique of the grain resistivity measurement in oxide varistor ceramics is suggested. For improvement of the measurement precision the linear extrapolation of the dependence of the differential electrical resistance on the reverse current density to $J^{-1}=0$ is applied. The single exponential voltage pulses were used for the measurements. This technique is applicable in the region of the current density of (10–500) A cm^{-2}, where the overheating of varistor sample by the exponential pulse with the time constant not more than 100 μs is insignificant. Such technique was verified for commercial ZnO varistors. The grain resistivity of $0.60\pm0.02\,\Omega$ cm at 293 K and of $3.40\pm0.13\,\Omega$ cm at 77 K were obtained. It indicates that the temperature coefficient of grain resistance in zinc oxide varistor ceramics in the temperature range (77–293) K is negative. On the basis of the experimental current–voltage characteristic of zinc oxide varistor and the measured grain resistivity, the contribution of the grain boundaries (excluding the grains) to the current–voltage characteristic of varistor is estimated. At current density higher than approximately 1000 A cm^{-2} the current–voltage characteristic of ZnO varistor is nearly linear, the voltage drop at the grain-boundary regions varies weakly with current and the electrical conduction in ZnO varistor ceramics is controlled by grains.

References

[1] M. Matsuoka, Discovery of ZnO varistors and their progress for the two decades, in: L.M. Levinson (Ed.), Advances in Varistor Technology. Ceramic Transactions, Vol. 3, American Ceramic Society, Schenectady, 1989, pp. 3–9.

[2] L.M. Levinson, Electronic ceramics: properties, devices and applications, Marcel Dekker Inc., New York, 1988.

[3] T.K. Gupta, Application of zinc oxide varistors, Journal of the American Ceramic Society 73 (1990) 1817–1840.

[4] D. Clarke, Varistor ceramics, Journal of the American Ceramic Society 82 (1999) 485–502.

[5] A.M.R. Senos, J.L. Baptista, Atmosphere effects in the grain boundary region of ZnO varistors, Journal of Materials Science Letters 3 (1984) 213–216.

[6] S. Bernik, N. Daneu, Characteristics of SnO_2-doped ZnO-based varistor ceramics, Journal of the European Ceramic Society 21 (2001) 1879–1882.

[7] S. Bernik, J. Bernard, N. Daneu, A. Recnik, Microstructure development in low-antimony oxide-doped zinc oxide ceramics, Journal of the American Ceramic Society 90 (2007) 3239–3247.

[8] A. Sedky, T.A. El-Brolossy, S.B. Mohamed, Correlation between sintering temperature and properties of ZnO ceramic varistors, Journal of Physics and Chemistry of Solids 73 (2012) 505–510.

[9] H.R. Philipp, L.M. Levinson, High-frequency and high-current studies of metal oxide varistors, Journal of Applied Physics 47 (1976) 3116–3121.

[10] H.R. Philipp, L.M. Levinson, Optical method for determining the grain resistivity in ZnO-based ceramic varistors, Journal of Applied Physics 47 (1976) 1112–1116.

[11] W.G. Carlson, T.K. Gupta, Improved varistor nonlinearity via donor impurity doping, Journal of Applied Physics 53 (1982) 5746–5753.

[12] F.A. Modine, R.B. Wheeler, Pulse response characteristics of ZnO varistors, Journal of Applied Physics 67 (1990) 6560–6566.

[13] Z.Y. Lu, Z.W. Chen, F.J. Yang, Voltage response of ZnO varistors to 8/20 μs surge current, Key Engineering Materials 280–283 (2005) 285–288.

[14] M. Houabes, R. Metz, Rare earth oxides effects on both the threshold voltage and energy absorption capability of ZnO varistors, Ceramics International 33 (2007) 1191–1197.

[15] S. Mahmud, M.J. Abdullah, G.A. Putrus, Increase in upturn power dissipation of surge suppressors due to highly defective nanostructure of zinc oxide, synthesis and reactivity in inorganic, Metal-Organic and Nano-Metal Chemistry 36 (2006) 59–64.

[16] A.B. Glot, Z.Y. Lu, Z.Y. Zhou, A.I. Ivon, Electrical properties of SnO_2 ceramic varistors withstanding high current pulses, Superficies y Vacio 24 (2011) 61–67.

[17] Z.Y. Lu, A.B. Glot, A.I. Ivon, Z.Y. Zhou, Electrical properties of new tin dioxide varistor ceramics at high currents, Journal of the European Ceramic Society 32 (2012) 3801–3807.

[18] A.I. Ivon, A.B. Glot, A.V. Gaponov, S.V. Mazurik, Grain resistivity and grain size in non-Ohmic oxide ceramics, Key Engineering Materials 132–136 (1997) 1289–1292.

[19] A.B. Glot, I.A. Skuratovsky, Non-Ohmic conduction in tin dioxide based varistor ceramics, Materials Chemistry and Physics 99 (2006) 487–493.

[20] R. Metz, D. Koumeir, J. Morel, J. Pansiot, M. Houabes, A. Hassanzadeh, Electrical barriers formation at the grain boundaries of Co-doped SnO_2 varistor ceramics, Journal of the European Ceramic Society 28 (2008) 829–835.

[21] M.A. Ramirez, W. Bassi, R. Parra, P.R. Bueno, E. Longo, J.A. Varela, Comparative electrical behavior at low and high current of SnO_2- and ZnO-based varistors, Journal of the American Ceramic Society 91 (2008) 2402–2404.

[22] Z.Y. Lu, Z. Chen, J.Q. Wu, SnO_2-based varistors capable of withstanding surge current, Journal of the Ceramic Society of Japan 117 (2009) 851–855.

[23] R. Metz, J. Pansiot, M. Hassanzadeh, Nanosecond reversible solid state switches capable of handling MJ of energy, Journal of the European Ceramic Society 32 (2012) 2443–2450.

[24] J. Hana, A.M.R. Senos, P.Q. Mantas, W. Cao, Dielectric relaxation of shallow donor in polycrystalline Mn-doped ZnO, Journal of Applied Physics 93 (2003) 4097–4103.

[25] A.C. Caballero, Hevia D. Fernandez, J. De Frutos, M. Peiteado, J.F. Fernandez, Bulk grain resistivity of ZnO-based varistors, Journal of Electroceramics 13 (2004) 759–763.

[26] A.I. Ivon, Parameters of ZnO grains in ZnO-based ceramics, Inorganic Materials 36 (2000) 1074–1077.

[27] M. El-Hofy, Grain boundary defects induced switching in Zn–Bi–Mo ceramic, Defect and Diffusion Forum 251–252 (2006) 13–20.

[28] R. Einzinger, Grain junction properties of ZnO varistors, Applications of Surface Science 3 (1979) 390–408.

[29] G.D. Mahan, L.M. Levinson, H.R. Philipp, Theory of conduction in ZnO varistor, Journal of Applied Physics 50 (1979) 2799–2812.

[30] L.K.J. Vanadamme, J.C. Brugman, Conduction mechanisms in ZnO varistor, Journal of Applied Physics 51 (1979) 4240–4244.

[31] G.E. Pike, Electronic properties of ZnO varistors: a new model, in: H.J. Leamy, G.E. Pike, C.H. Seager (Eds.), Grain Boundaries in Semiconductors. Proceedings of the Materials Research Society Annual Meeting, Elsevier Science Publishing Company, Inc., Boston, MA, 1982, pp. 369–379.

[32] G. Blatter, F. Greuter, Electrical breakdown at semiconductor grain boundaries, Physical Review B: Condensed Matter and Materials Physics 34 (1986) 8555–8572.

[33] L.M. Levinson, H.R. Philipp, Low-temperature ac properties of metal-oxide varistors, Journal of Applied Physics 49 (1978) 6142–6146.

[34] E. Olsson, G.L. Dunlap, Characterization of individual interfacial barriers in ZnO varistor material, Journal of Applied Physics 66 (1989) 3666–3675.

[35] S.T. Tan, B.J. Chen, X.W. Sun, W.J. Fan, H.S. Kwok, X.H. Zhang, S.J. Chua, Blueshift of optical band gap in ZnO thin films grown by metal-organic chemical-vapor deposition, Journal of Applied Physics 98 (2005) 013505 (5 pages).